Targeted Delivery of CXCL9 and OX40L by Mesenchymal Stem Cells Elicits Potent Antitumor Immunity

Pan Yin,[1,2] Liming Gui,[1,2] Caihong Wang,[1,2] Jingjing Yan,[1,2] Min Liu,[1,2] Lu Ji,[1,2] You Wang,[3] Bin Ma,[1,2] and Wei-Qiang Gao[1,2]

[1]State Key Laboratory of Oncogenes and Related Genes, Renji-Med-X Clinical Stem Cell Research Center, Ren Ji Hospital, School of Medicine and School of Biomedical Engineering, Shanghai Jiao Tong University, Shanghai 200127, China; [2]Med-X Research Institute, Shanghai Jiao Tong University, Shanghai 200030, China; [3]Department of Obstetrics and Gynecology, Renji Hospital, School of Medicine, Shanghai Jiao Tong University, Shanghai 200127, China

Major obstacles in immunotherapies include toxicities associated with systemic administration of therapeutic agents, as well as low tumor lymphocyte infiltration that hampers the efficacies. In this study, we report a mesenchymal stem cell (MSC)-based immunotherapeutic strategy in which MSCs specifically deliver T/natural killer (NK) cell-targeting chemokine CXCL9 and immunostimulatory factor OX40 ligand (OX40L)/ tumor necrosis factor superfamily member 4 (TNFSF4) to tumor sites in syngeneic subcutaneous and azoxymethane (AOM)/dextran sulfate sodium (DSS)-induced spontaneous colon cancer mouse models. This approach generated potent local antitumor immunity by increasing the ratios of tumor-infiltrating CD8+ T and NK cells and production of antitumor cytokines and cytolytic proteins in the tumor microenvironment. Moreover, it improved the efficacy of programmed death-1 (PD-1) blockade in a syngeneic mouse model and significantly suppressed the growth of major histocompatibility complex class I (MHC class I)-deficient tumors. Our MSC-based immunotherapeutic strategy simultaneously recruits and activates immune effector cells at the tumor site, thus overcoming the problems with toxicities of systemic therapeutic agents and low lymphocyte infiltration of solid tumors.

INTRODUCTION

Chimeric antigen receptor (CAR)-modified T cells and immune regulatory checkpoint blockade are at the forefront of immunotherapy for cancers of various histological types.[1,2] Antibodies targeting T cell inhibitory receptors programmed death-1 (PD-1) or cytotoxic T lymphocyte-associated protein 4 (CTLA-4) can result in impressive tumor control in patients. However, in most cases the therapeutic efficacy is limited by many obstacles such as low infiltration of immune effector cells in solid tumors.[3,4] Weak tumor expression of T helper 1 (Th1)-type chemokines such as CXCL9 and CXCL10 that mediate effector T cell and natural killer (NK) cell migration may predict a poor survival rate and/or clinical response to anti-PD-1/programmed death-ligand 1 (PD-L1) therapy.[4–6] These results suggest that use of Th1-type chemokines may serve as a potential therapeutic strategy

to overcome the problems of low lymphocyte infiltration or lymphocyte exclusion in many tumors. However, a chemotactic gradient needs to be established from the tumor to achieve therapeutic effects, and an increase in the plasma concentration of these chemokines impairs the antitumor effects of other immunotherapies,[7] implying that systemic administration of these chemokines would not be an option. Moreover, intratumoral administration of agents remains a challenge in routine clinical practice. Additionally, systemic administration of high-dose immunomodulatory agents may cause serious side effects; for example, increasing cases of fatal immune checkpoint inhibitor-associated myocarditis are being reported.[8–10] Therefore, efficient immunotherapies specifically targeting tumors are urgently needed.

Mesenchymal stem cells (MSCs) are emerging as promising cellular vehicles that possess an intrinsic preferential migratory ability toward a number of different tumor types upon systemic administration.[11–13] Their availability from many different adult tissues, ease of expansion in culture, the ability to avoid immune rejection, and their tumor-tropic migratory properties and long lifespan at the site of residence make MSCs a great resource for cell-based therapy. Commonly used types of MSCs are bone marrow-derived MSCs (BM-MSCs), umbilical cord blood-derived MSCs (UCB-MSCs), and adipose tissue-derived MSCs (AT-MSCs). However, the isolation procedures of BM-MSCs and UCB-MSCs are complex and inefficient. Adipose tissue is a promising alternative to them, since it contains a much higher frequency of MSCs, and the tissue is more accessible and easier to collect.[14] As compared to BM-MSCs, AT-MSCs can be cultured for a longer period *in vitro*[14] and express higher levels of chemokine receptors, implicating a better migration capacity.[15] Additionally, regarding the source of autologous stem cells for personalized cell-
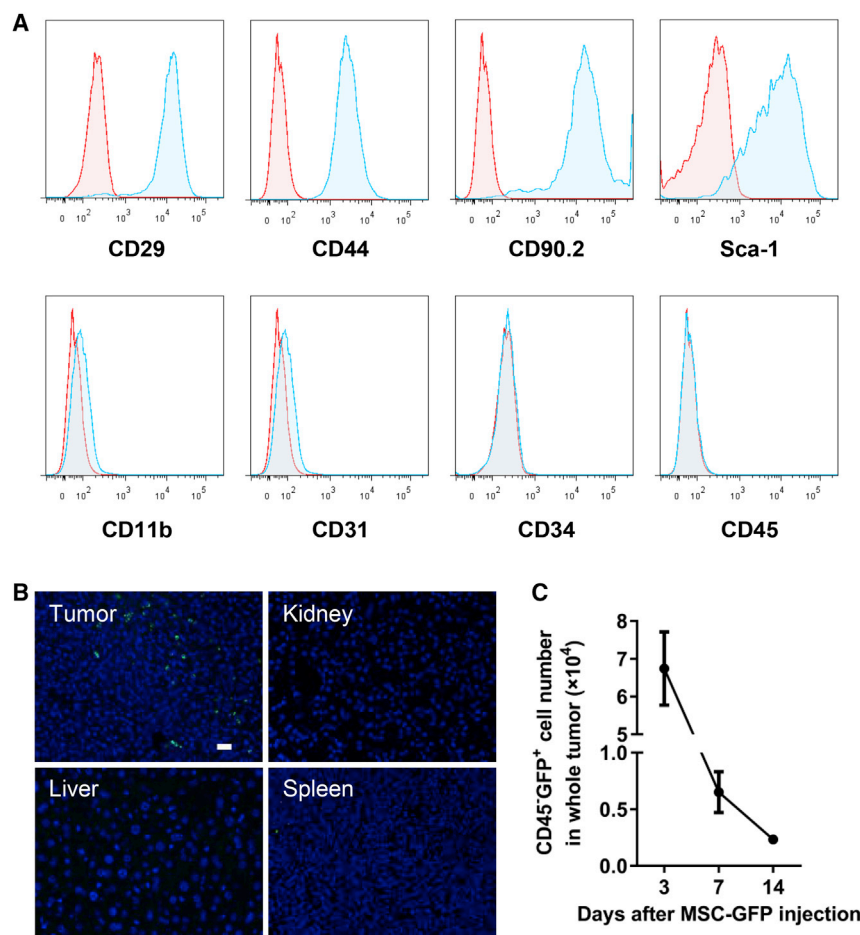
A

B

C

Figure 1. AT-MSCs Selectively Migrate to and Reside in Tumors

(A) Characterization of AT-MSCs isolated from BALB/c mice by FACS. (B) CT26 tumors and different organs were collected 1 week after MSC injection (0.5×10^6 cells/mouse), and MSC-GFP was detected by immunofluorescent staining (GFP, green) in tissue sections. Nuclei were stained with DAPI (blue). Scale bars, 20 μm. (C) Numbers of CD45⁻GFP⁺ MSCs in whole tumors at indicated time points after MSC injection were measured (n = 3).

based therapy, AT-MSCs bear minimal risk to the donor and no ethical concerns.

By utilizing the tumor-homing ability of MSCs, we hypothesize that targeted delivery of a Th1-type chemokine such as CXCL9 and an immunostimulatory factor such as OX40 ligand (OX40L)/tumor necrosis factor superfamily member 4 (TNFSF4)[16] by MSCs can simultaneously recruit effector T and NK cells to the tumor microenvironment and activate them, which generates a more localized and sustained immune response against tumor cells. In the current study, we address the potentials of AT-MSCs to serve as vehicles of chemokines and immunostimulatory factors to treat colorectal cancer in mouse models.

RESULTS

Specific Migration and Homing of AT-MSCs to Tumor Sites in a Syngeneic Model

To test whether AT-MSCs can serve as an ideal vehicle for delivery of therapeutic molecules to tumor sites, we first isolated and characterized mouse AT-MSCs. These cells expressed MSC-specific markers, including CD29, CD44, CD90, and Sca-1, but they lacked myeloid cell marker CD11b, endothelial cell marker CD31, hematopoietic or endothelial progenitor cell marker CD34, or leukocyte marker

CD45 (Figure 1A; Figure S1A), indicating a high purity of the AT-MSCs. The ability of the isolated MSCs to undergo osteogenic differentiation was also verified (Figure S1B). MSCs of BALB/c mice origin were transduced to stably express GFP by lentiviruses, and an injection of 0.5×10^6 GFP-labeled MSCs was given to the BALB/c mice bearing subcutaneous CT26 tumors systemically via the tail vein. One week after MSC injection, tumors and other organs were retrieved and processed for GFP expression by immunostaining tissue sections. GFP⁺ cells were enriched in the subcutaneous CT26 tumor, but not other organs, including the kidney, spleen, and liver (Figure 1B). GFP⁺ MSCs remained detectable in the tumors 2 weeks after intravenous (i.v.) injection, although there was a gradual decrease in cell numbers (Figure 1C). To test the tumorigenicity of MSCs, different doses of AT-MSCs of BALB/c origin were injected subcutaneously to BALB/c mice. No palpable tumors were observed for a period of 60 days in mice injected with up to 5×10^6 MSCs (Figure S1C). These results reveal that systemically administered AT-MSCs are able to specifically migrate to and reside in tumors without affecting normal organs, supporting their potential as a safe and efficient drug vehicle to target tumors.

Delivery of CXCL9 and OX40L by AT-MSCs Leads to Tumor Regression

Tumor lymphocyte infiltration is a crucial factor determining the outcome of immunotherapy. Th1-type chemokines such as CXCL9 and CXCL10 were shown to be important for the recruitment of NK and T cells,[5] suggesting a therapeutic potential of these chemokines. To assess the antitumor effects of these chemokines, we generated CT26 mouse colon cancer cell lines overexpressing CXCL9 and another chemokine, CCL3, by lentiviral transduction[17] (Figure S2A). Tumor cells overexpressing these chemokines did not show any change in proliferation in vitro (Figure S2B), while tumor growth in vivo was suppressed by overexpression of these two chemokines, with CXCL9 showing a more significant inhibition (Figure S2C). Fluorescence-activated cell sorting (FACS) analysis of tumor lymphocyte infiltration showed that CXCL9 overexpression significantly
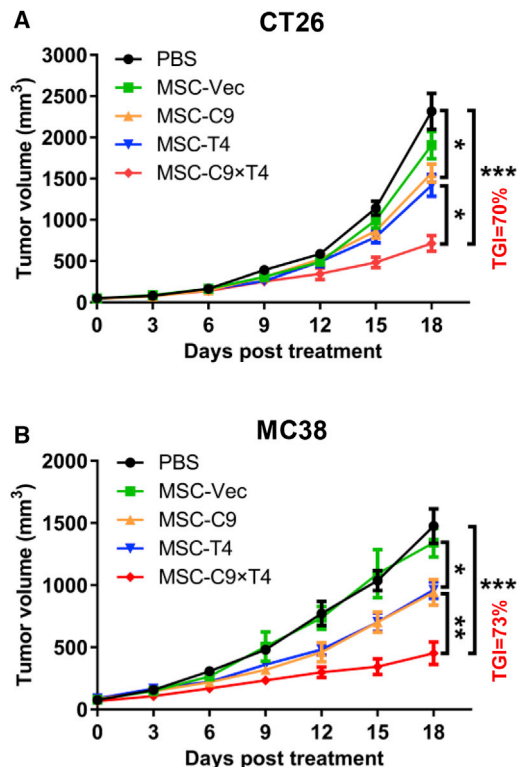
Figure 2. Delivery of CXCL9 and OX40L by AT-MSCs Leads to Tumor Regression

(A and B) CT26 (A) and MC38 (B) tumors were established subcutaneously. 0.5×10^6 MSC-Vec, MSC-C9 (CXCL9), MSC-T4 (OX40L), MSC-C9 × T4 cells, or PBS was administered by i.v. injection every 4 days for a total of four times. Tumor growth was recorded over time (n = 6 mice per group).

increased the number of tumor-infiltrating CD8$^+$ T and NK cells (Figure S2D). CXCL9 elicited a stronger recruitment of major antitumor effector cells, including CD8$^+$ T and NK cells, as compared to CCL3, in agreement with its stronger antitumor effect. These data indicate that the antitumor effect of CXCL9 may depend on the increased immune effector cells rather than a direct inhibition of tumor cell proliferation. We also found a positive correlation between CXCL9 expression and survival rate in human colorectal cancer patients (Figure S2E) using the PROGgeneV2-Pan Cancer Prognostics Database,[18] which is consistent with a previous study.[19] Taken together, these results support the antitumor potential of CXCL9.

To further stimulate the tumor-resident or the newly recruited antitumor lymphocytes, we sought to use another immunostimulatory factor in addition to CXCL9 for our therapeutic strategy. After initial screening of several potential antitumor cytokines from the interleukin (IL) and TNF family, we focused on IL-36β and OX40L/TNFSF4, two factors recently reported to stimulate T and NK cell-mediated antitumor responses and that hold great therapeutic promise.[16,20,21] CT26 tumor cells overexpressing IL-36β and OX40L/TNFSF4 were generated by lentiviral transduction (Fig-

ure S3A). Membrane-bound expression of OX40L was also verified by flow cytometry (Figure S3B). Overexpression of these factors did not influence tumor cell proliferation *in vitro* but showed tumor-suppressive effects *in vivo*, suggesting that their antitumor functions may depend on the immune system (Figures S3C and S3D). OX40L showed stronger inhibitory effects on tumor growth than did IL-36β. Additionally, considering that OX40 agonists have been reported to exhibit promising potential in many pre-clinical tumor models,[16] we used OX40L together with CXCL9 in the following studies.

Using lentiviral transduction, we generated mouse AT-MSCs overexpressing the immunomodulatory factors CXCL9 (MSC-C9), OX40L/TNFSF4 (MSC-T4), or both (MSC-C9 × T4) or empty vector (MSC-Vec). Protein expression was first confirmed by western blotting (Figure S4A). Secretion of CXCL9 and membrane-bound expression of OX40L were further evaluated by enzyme-linked immunosorbent assay (ELISA) and flow cytometry, respectively (Figures S4B and S4C). Production of CXCL9 or OX40L by MSCs overexpressing both genes was equivalent to that of cells overexpressing either factor alone. The amount of secreted CXCL9 was always within the range of 4,500–6,500 pg/10^6 cells after 48-h culture for all experiments as determined by ELISA (Figure S4B). Consistent with the observation with wild-type MSCs (Figure S1C), lentivirally transduced MSCs did not show any tumorigenic ability even after 120 days upon subcutaneous inoculation (Figure S4D). BALB/c mice bearing CT26 tumors or C57BL/6 mice with MC38 tumors received four i.v. injections of 0.5×10^6 engineered MSCs from corresponding strains or PBS. MSCs carrying CXCL9, OX40L, and both all significantly reduced tumor growth compared to the PBS and MSC-Vec treatments (Figures 2A and 2B). In both tumor models, MSC-C9 × T4 treatment resulted in at least 70% tumor growth inhibition (TGI), which was higher than MSC-C9 or MSC-T4. During the experiments, we did not observe any MSC treatment-associated side effects in mice, including body weight changes, fatigue, and loss of appetite.

To examine the effects of MSC therapy on tumor immunity, we performed FACS analysis of the major immune cells in CT26 and MC38 tumor models treated with engineered MSCs. The percentages of CD4$^+$ T cells in total live cells were not changed by MSCs overexpressing CXCL9, OX40L, or both (Figure 3A; Figure S5A). As compared with PBS or MSC-Vec controls, the ratios of both CD8$^+$ T and NK cells were elevated in tumors treated with MSC-C9, MSC-T4, and MSC-C9 × T4, with the MSC-C9 × T4 group exhibiting the highest level. Moreover, higher proportions of CD8$^+$ T and NK cells were positive for the expression of the cytolytic enzyme granzyme B (Gzmb) in tumors treated with MSCs overexpressing CXCL9, OX40L, or both, suggesting an enhancement of antitumor capacity by these cells (Figure 3B; Figure S5B). In general, MSC-C9 × T4 therapy showed a higher ability to promote tumor infiltration of CD8$^+$ T and NK cells as well as Gzmb expression in these cells than did MSC-C9 and MSC-T4 treatments, although not statistically significant in all cases. Accordingly, quantitative PCR (qPCR) analysis revealed an upregulation of mRNA expression of other antitumor cytokines, including interferon (IFN)-β1 (*Ifnb1*), IFN-γ (*Ifng*), IL-2 (*Il2*), and IL-15 (*Il15*) in the MC38 tumors treated with MSCs
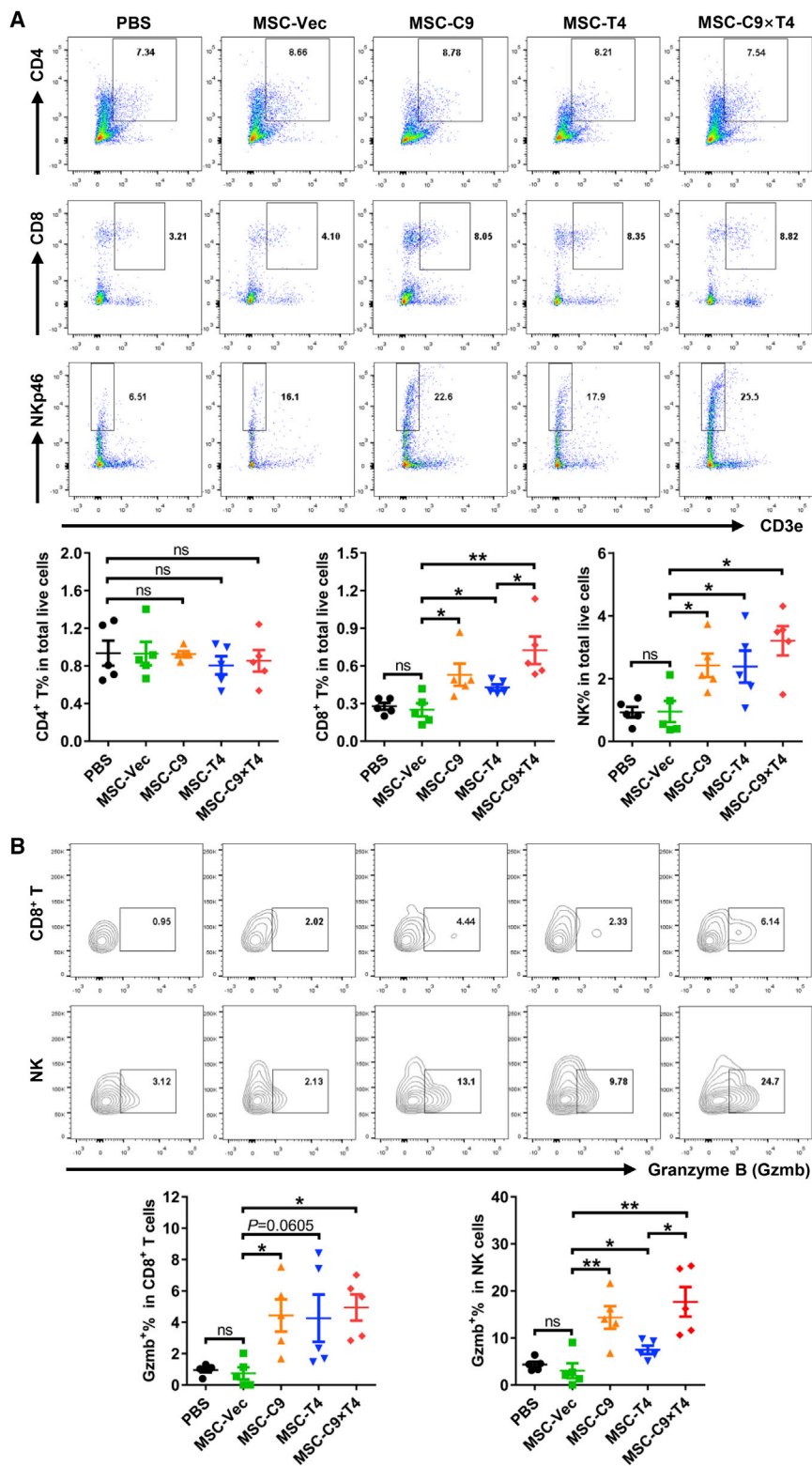
Figure 3. Delivery of CXCL9 and OX40L by AT-MSCs Shapes CT26 Tumor Immune Microenvironment

(A) Tumor-infiltrating CD4$^+$ T, CD8$^+$ T, and NK cells were analyzed by flow cytometry 3 days after the last injection of MSCs in CT26 tumor model (gate on CD45$^+$) (n = 5). (B) Expression of granzyme B (Gzmb) in CD8$^+$ T and NK cells was analyzed by flow cytometry (n = 5). *p < 0.05, **p < 0.01. ns, not significant.
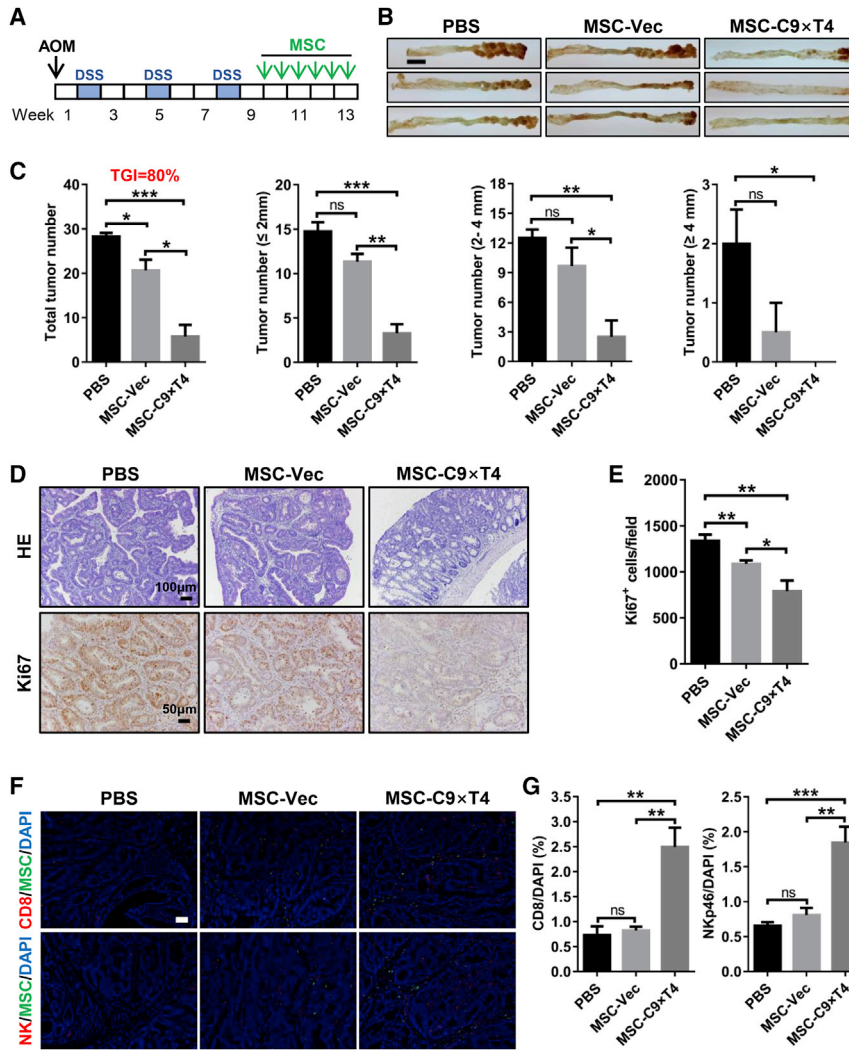
Figure 4. MSC-C9 × T4 Therapy Inhibits AOM/DSS-Induced Colorectal Tumor Progression

(A) Scheme of AOM/DSS administration and treatment schedule. 0.5×10^6 MSCs were given for each injection. (B) Representative images of gross appearance of mouse colon tumors. Scale bar, 5 mm. (C) Statistics of tumor numbers in different size ranges (n = 3–4 mice per group). (D) H&E staining and Ki67 immunohistochemistry of mouse colons. (E) Statistics of Ki67+ cell numbers on tissue sections (n = 8). (F) Immunostaining of CD8+ cells (anti-CD8), NK cells (anti-NKp46), and MSCs (anti-GFP) in colorectal tumors. Scale bar, 50 μm. (G) Statistics of CD8+ and NK cell ratios (n = 5). *p < 0.05, **p < 0.01, ***p < 0.001. ns, not significant.

overexpressing immunomodulatory factors (Figure S6). Furthermore, MSC-C9 × T4 also attenuated the presence of immune inhibitory molecules, including PD-1 and Tim-3 on CD8+ T cells, indicating a less exhausted phenotype (Figure S7). As opposed to the observations in the tumors, T cells were not significantly affected in the spleens (Figure S8). Interestingly, there was a decrease in NK cells in the spleens of mice that received MSC-C9 × T4 therapy, possibly due to an induced migration of NK cells from the spleens to tumors. Taken together, these results indicate that MSC-C9 × T4 treatment triggers a local antitumor immune response mainly through upregulation of both infiltration and activity of CD8+ T and NK cells.

MSC-C9 × T4 Therapy Suppresses Colitis-Associated Cancer Progression

It is well accepted that individuals with chronic intestinal inflammatory disease are at high risk for developing colorectal cancer.[22,23] We further tested the therapeutic effects of our MSC-based immunotherapy in a spontaneous model of colitis-associated cancer.[24,25] A mouse colorectal tumor model was established using azoxymethane (AOM) and dextran sulfate sodium (DSS) (Figure 4A). MSC therapy started from the last week of the DSS treatment cycle when apparent tumors had formed,[24,25] in order to explore the therapeutic rather than prophylactic effects, and a total of six injections of 0.5×10^6 MSCs each were given during a 4-week therapeutic period (Figure 4A). MSC-C9 × T4 exhibited a drastic inhibition of colorectal tumor formation, and almost no identifiable tumors were observed in one of the treated mice (Figures 4B and 4C). As compared to the syngeneic models of CT26 or MC38, the therapeutic effects were more remarkable in this clinically relevant spontaneous tumor model with a TGI rate of 80%. In sharp contrast, treatment with a combination of anti-PD-1 and anti-CTLA-4 antibodies did not show any significant therapeutic effects in this AOM/DSS-induced tumor model (Figure S9). Histology and immunohistochemistry also showed that the structure of colonic crypts was largely preserved, and the dysplastic grade and the number of Ki67+ proliferating epithelial cells (MSC-C9 × T4 versus PBS, p = 0.0011; MSC-C9 × T4 versus MSC-Vec, p = 0.0285) were both reduced in treated mice (Figures 4D and 4E). The presence of GFP+ MSCs in the colorectal tumors was confirmed by immunofluorescence (Figure 3F). Consistent with previous findings in the subcutaneous tumor model, MSC-C9 × T4 therapy increased the numbers of CD8+ cells and NK cells in the spontaneous colorectal tumors (Figures 4F and 4G).

MSC-C9 × T4 Treatment Enhances the Efficacy of PD-1 Blockade

Since lymphocyte exclusion is one of the most important factors limiting the response to immune checkpoint blockade and our MSC therapy was able to efficiently increase T and NK cell numbers in tumors, we next explored whether MSC-C9 × T4 could improve the efficacy of immune checkpoint blockade. In the CT26 tumor model that
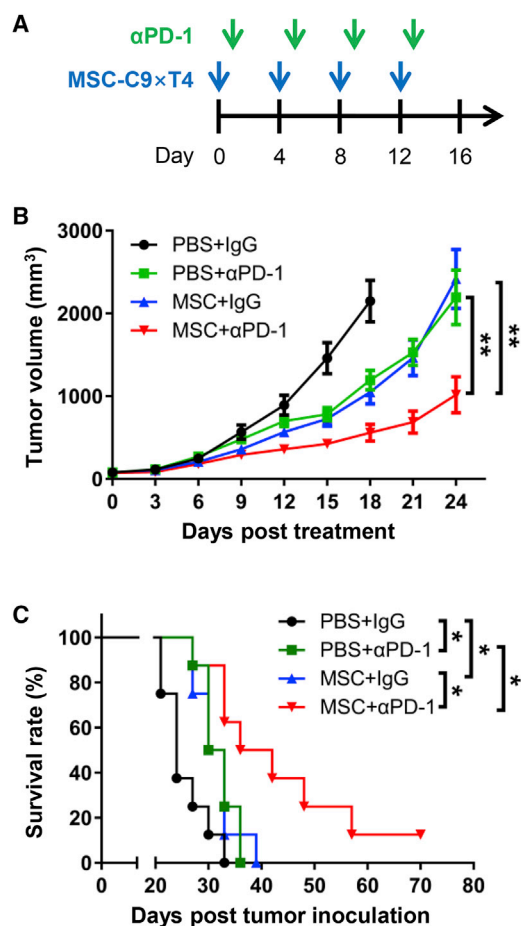
Figure 5. MSC-C9 × T4 Treatment Enhances the Efficacy of PD-1 Blockade
(A) Scheme of MSC-C9 × T4 and anti-PD-1 antibody (αPD-1) treatment schedule.
(B) Growth of CT26 tumors following treatments was recorded (n = 7–8 mice per group). (C) Survival rate of CT26 tumor-bearing BALB/c mice treated with engineered MSCs and αPD-1. *p < 0.05, **p < 0.01.

was the least sensitive to MSC therapy (Figures 2 and 4C), we treated the mice with anti-PD-1 antibody, MSC-C9 × T4, or a combination of both (Figure 5A). Both anti-PD-1 antibody and MSC-C9 × T4 treatment repressed tumor growth (Figure 5B) and improved mouse survival (anti-PD-1 versus immunoglobulin G [IgG], p = 0.0114; MSC-C9 × T4 versus PBS, p = 0.0131) (Figure 5C). As compared with single therapies, combination therapy indeed resulted in a significantly higher tumor regression grade (combination versus anti-PD-1, p = 0.0025; combination versus MSC-C9 × T4, p = 0.0060) and survival rate (combination versus anti-PD-1, p = 0.0300; combination versus MSC-C9 × T4, p = 0.0192) (Figures 5B and 5C), indicating that MSC-C9 × T4 treatment improved the antitumor efficacy of PD-1 blockade.

MSC-C9 × T4 Therapy Restrains the Growth of MHC Class I-Deficient Tumors

Loss of major histocompatibility complex class I (MHC class I) expression on the tumor cell surface promotes tumor escape

from adaptive immune system-dependent surveillance or immunotherapy.[26,27] In this case, the NK cell-mediated innate immune response seems to be an appropriate way to eliminate the MHC class I-deficient tumor cells. It was observed that our MSC therapy stimulated NK cells in the tumors. Therefore, we further sought to examine whether this treatment could also exhibit antitumor activity against MHC class I-deficient tumor cells. We generated MHC class I-deficient MC38 cells using CRISPR-mediated knockout (KO) of β_2-microglobulin (*B2m*) followed by cell sorting. The control MC38 cells transduced with single-guide RNA (sgRNA) against the LacZ gene (sgLacZ) were positive for H-2Kb/H-2Db (MHC class I), whereas the B2m-KO cells were MHC class I-negative *in vitro* even in the presence of IFN-γ (Figure S10A) as well as *in vivo* (Figure 6A). The proliferation of these two cell lines showed no difference *in vitro* (Figure S10B), but the B2m-KO MC38 tumors showed a much higher growth rate in mice than did the control sgLacZ MC38 tumors (Figure 6B). MSC-C9 × T4 significantly restrained MHC class I-deficient MC38 tumor growth (Figures 6C and 6D). Depletion of NK cells by anti-NK1.1 antibody abrogated the antitumor effect of MSC therapy (Figure 6D), indicating that NK cells are the downstream effector cells for the MSC-C9 × T4-mediated immune response against MHC class I-deficient tumors. Surprisingly, depletion of CD8$^+$ cells also eliminated the therapeutic effect on these MHC class I-deficient tumor cells, which might be partly due to the outgrowth of the very few MHC class I-positive cells (Figure 6E) and/or elimination of CD8$^+$ NK cells besides CD8$^+$ T cells upon anti-CD8 antibody treatment. Notably, mRNA expression of cytolytic enzyme Gzmb and antitumor cytokines, including IFN-β (*Ifnb1*), IFN-γ (*Ifng*), and IL-15 (*Il15*), in the MHC class I-deficient tumors was elevated by MSC-C9 × T4 treatment, but abrogated by anti-CD8 or anti-NK1.1 antibody (Figure S11), implying that loss of antitumor cytokines might contribute to the depleting antibody-induced loss of the antitumor effect. Another antitumor cytokine IL-2 (*Il2*) was downregulated by the depleting antibodies, although not influenced by MSC therapy, while expression of the immunosuppressive cytokine IL-10 (*Il10*) did not change in all conditions. These data suggest that the above-examined antitumor proteins are involved in the antitumor actions of MSC-C9 × T4 and counteractive effects of CD8 and NK cell-depleting antibodies.

DISCUSSION

Recent breakthroughs in cancer immunotherapies have dramatically strengthened our fight against cancer. However, the inconsistent responsiveness and limitations of current therapeutic strategies are leading us to develop more specific and efficacious immunotherapies. One major concern is the toxicity associated with systemic administration of immunotherapeutic agents such as cytokines and antibodies. For example, increasing cases of myocarditis-caused death in cancer patients treated with immune checkpoint inhibitors are being reported.[9,10] Therefore, targeted delivery of immunomodulatory agents to tumors may be a potential solution to solve this problem. By taking advantage of the tumor-homing ability of MSCs, we demonstrated clearly that specific chemokines
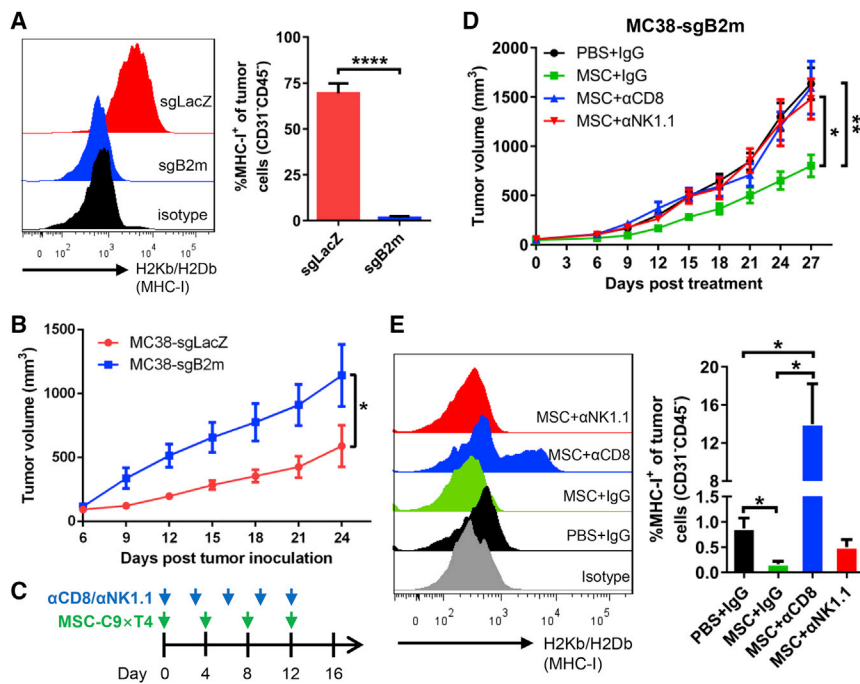
Figure 6. MSC-C9 × T4 Therapy Inhibits the Growth of MHC Class I-Deficient Tumors

(A) FACS analysis of MHC class I (H-2Kb/H-2Db) expression on control (sgLacZ) and B2m-KO (sgB2m) MC38 cells (CD31⁻CD45⁻) isolated from subcutaneous tumors (n = 4). (B) C57BL/6 mice were inoculated with WT or B2m-KO (MHC class I⁻) MC38 cells. Tumor growth was measured over time (n = 4 mice per group). (C) Scheme of MSC-C9 × T4 and anti-CD8/anti-NK1.1 (αCD8/αNK1.1) depleting antibody treatment. (D) C57BL/6 mice bearing B2m-KO (MHC class I⁻) MC38 tumors were treated with MSC-C9 × T4 and αCD8/αNK1.1 depleting antibody. Tumor growth was recorded over time (n = 5–7 mice per group). (E) FACS analysis of MHC class I expression on MC38 cells (CD31⁻CD45⁻) isolated from subcutaneous tumors on day 27 after treatment (n = 4). *p < 0.05, **p < 0.01, ****p < 0.0001.

and immunostimulatory factors can be successfully delivered to tumor sites in both syngeneic and spontaneous AOM/DSS-induced colon cancer mouse models via a systemic route and generated a potent localized antitumor immune response without affecting other organs.

Our MSC-based immunotherapy actively inflames tumors with immune effector cells, including T and NK cells, and shows promising therapeutic effects in colorectal tumors, one of the least immunogenic cancer types.[28] Analysis of tumor samples from patients treated with immunotherapeutic agents such as checkpoint inhibitors and/or cancer vaccines in previous studies shows that patients with pre-existing T cells were more likely to exhibit clinical responses.[29,30] This finding implies that reactivation of T cells or other immune effector cells already present within the tumor immune microenvironment is critical for better efficacy of many immunotherapies.[31] However, many solid tumors do not show a T cell-inflamed phenotype.[28] Tumors may develop barriers for T cell homing through various mechanisms, such as reduction of effector cell-recruiting chemokines by oncogenic pathways or epigenetic silencing, and recruitment of immunosuppressive cells, including MDSCs that in turn inhibit the infiltration of effector cells.[3,4,32] Targeting the oncogenic or epigenetic pathways or immunosuppressive cells might restore T cell infiltration, but the treatments may be individual patient-dependent and require complicated molecular diagnosis. In this study, by using chemokine-overexpressing MSCs, we provide a straightforward strategy to shape the tumor immune microenvironment into the T and NK cell-infiltrated state regardless of mechanisms responsible for the non-T cell-inflamed phenotype. The beauty of this method is that it may potentially benefit a much broader range of cancer patients pursuing immunotherapy.

The current study also shows that use of immunostimulatory OX40L further adds up to the antitumor effects of MSCs overexpressing chemokine CXCL9. In addition to the more widely used immune checkpoint inhibitors such as anti-PD-1/PD-L1 and anti-CTLA-4 antibodies to relieve the immunosuppression, an alternative way to enhance antitumor activity is the activation of costimulatory receptors, among which one of the most promising targets is the TNF receptor superfamily member TNFRSF4/OX40.[16,33] Several OX40-stimulating monoclonal antibodies have undergone clinical trials.[33,34] The expression of surface-bound immunostimulatory ligands such as OX40L in MSCs provides more localized and specific effects than using agonistic antibodies that exert diffusive actions.

Our established MSC system may serve as a versatile platform to deliver any therapeutic genes. In a recent study, CAR-T cells were engineered to secrete PD-1-blocking single-chain variable fragments (scFvs) to improve the therapeutic effects.[35] MSCs can also serve as an ideal vehicle for such secreted immune checkpoint blocking scFvs, which will enhance the antitumor effects of other chemokines and immunostimulatory factors. The synergistic effects of cytokines and agonistic and blocking antibodies have been extensively studied.[16,36,37] By defining the optimal combinations of targets, we will be able to express selected transgenes in our MSC-based platform to achieve maximum therapeutic outcomes.

Another striking advantage of our MSC-based therapy is its ability to suppress the growth of MHC class I-negative tumors that are notorious for their resistance to adaptive immunity-mediated treatment such as cancer vaccines and CAR-T cells. Downregulation of membrane MHC class I expression on tumor cells allows tumor cells to escape from T cell killing.[26,27] Strategies such as IFN-γ treatment to increase tumor MHC class I expression would result in an enhanced T cell response in cancer patients.[38] However, it would be challenging to regain normal antigen presentation by

MHC class I when irreversible genetic aberrations/mutations in relevant genes such as *B2M* occur. In this regard, our MSC-based immunotherapy represents a promising and more direct strategy to eradicate MHC class I-negative tumors by mobilizing NK cells and bypassing the MHC class I/T cell-mediated adaptive immunity.

One major safety issue related to stem cell-based therapy is the incidence of cell transformation and tumor formation. However, there has not been enough evidence for the tumorigenicity of MSCs expanded *in vitro*. We did not observe any tumor formation by mouse AT-MSCs upon subcutaneous implantation in syngeneic mice (Figures S1C and S4D), which is consistent with a previous report showing that subcutaneous implantation of human UC-MSCs in immunodeficient mice did not lead to any tumor formation 2 months following implantation.[39] When given systemically via tail veins, AT-MSCs did not show any tumor-promoting effects in the subcutaneous tumor models (Figures 2A and 2B). More importantly, based on current clinical trial outcomes, MSC therapy appears to be safe in the treatment of disease other than cancer.[40,41] With regard to the potential use of MSCs for cancer treatment, caution needs to be taken, as both inhibiting and promoting effects of AT-MSCs on tumor cell growth and migration have been reported depending on cancer types,[42,43] although the predominant action of the engineered AT-MSCs might be anti-tumor. Especially in our AOM/DSS-induced spontaneous colorectal cancer model, AT-MSCs transduced with empty vector showed moderate but significant tumor-inhibiting effects (Figure 3C). This might be due to the growth-inhibiting or anti-angiogenic function of MSCs either through paracrine factors or cell-cell contact,[44–46] rather than an immunomodulating effect since neither CD8^{+} nor NK cells were affected by MSC-Vec (Figure 3G). More efforts are warranted in the future to verify the safety of AT-MSCs before applying them for the treatment of a specific type of cancer. One potential approach to further guarantee the safety of stem cell-based therapy in the future is the use of an inducible suicide system to eliminate the engineered stem cells after therapy.[47]

Taken together, in addition to current popular immunotherapies such as CAR-T cell and checkpoint inhibition, we have established a versatile and efficacious MSC-based platform combining specific antitumor chemokines and immunostimulatory factors. This MSC-based immunotherapy could break the lymphocyte-excluding barrier of tumors and holds great promises for the treatment of a broad range of cancers, regardless of the tumor lymphocyte infiltration conditions.

MATERIALS AND METHODS
Cell Lines
CT26 and MC38 cells are murine colon adenocarcinoma cells derived from BALB/c and C57BL/6 mice, respectively. CT26 and MC38 cells were cultured in RPMI 1640 and DMEM, respectively, supplemented with 10% fetal bovine serum (FBS) and 1% penicillin/streptomycin.

Cell lines were authenticated by Shanghai Biowing Applied Biotechnology using short tandem repeat analysis and routinely tested for mycoplasma.

MHC class I-deficient tumor cells were generated by CRISPR-mediated KO of *B2m*. Briefly, MC38 cells were transduced with lentiviruses expressing Cas9 and two sgRNA sequences targeting *B2m* (sgB2m #1, 5′-ATTTGGATTTCAATGTGAGG-3′; #2: 5′-ACTCACTCTGGA TAGCATAC-3′). Lentiviral vectors used for Cas9 and sgRNA expression were lentiCas9-Blast (Addgene plasmid #52962) and lentiGuide-Puro (Addgene #52963).[48] After antibiotic selection, MC38-sgB2m was stimulated with recombinant mouse IFN-γ (BioLegend) for 24 h and then sorted using FACSAria II (BD Bioscience) for three rounds to enrich H-2Kb/H-2Db (MHC class I)-negative MC38 cells.

Antibodies
The antibodies used for flow cytometry were purchased from BD Biosciences, BioLegend, or eBioscience. Antibodies used for western blotting were anti-CCL3 (R&D Systems), anti-CXCL9 (Abcam), anti-Myc-tag (Cell Signaling Technology), anti-OX40L (Abcam), and anti-GAPDH (Abcam). Antibodies used for immunofluorescence were anti-GFP (Abcam), anti-CD8a (BioLegend), and anti-NKp46 (CD335) (BioLegend).

The immune checkpoint blocking antibodies anti-PD-1 (clone RMP1-4) and anti-CTLA-4 (clone 9D9), and antibodies against CD8 (clone 2.43) and NK1.1 (clone PK136) for *in vivo* depletion of CD8 and NK cells, were purchased from Bio X Cell. All of these antibodies (anti-PD-1, 200 μg/mouse; anti-CTLA-4, 100 μg/mouse; anti-CD8, 200 μg/mouse; anti-NK1.1, 200 μg/mouse) were administered via the intraperitoneal (i.p.) route.

Isolation, Culture, and Identification of MSCs from Mouse Adipose Tissue
AT-MSCs were isolated from the mouse subcutaneous adipose tissue using collagenase type I (Thermo Fisher Scientific) digestion and plastic adherence technique as described,[49] Cells were plated in α-minimum essential medium (α-MEM) supplemented with 10% FBS and 1% penicillin/streptomycin.

To ascertain the *in vitro* differentiation ability, MSCs of the third passage were cultured in osteogenic differentiation medium (Cyagen Biosciences). To observe the calcium deposition, the differentiated cells were fixed with 4% paraformaldehyde and stained with alizarin red S.

Lentivirus Production and Transduction in MSCs
cDNAs were cloned into lentiviral vectors. Lentiviruses were produced and titrated by OBiO Technology (Shanghai). MSCs were infected with lentiviruses at a multiplicity of infection (MOI) of 60 in the presence of 8 μg/mL polybrene (Sigma-Aldrich). All lentivectors contained GFP, and a transduction efficiency of >90% in MSCs was validated by GFP expression under microscopy before use. Successful expression of CXCL9 and OX40L in MSCs was regularly validated by ELISA and FACS, respectively.

In Vitro Cell Proliferation Assay

Tumor cell proliferation was assessed by Cell Counting Kit-8 (CCK-8) (Dojindo, Japan) according to the manufacturer's instructions. Absorbance was measured using a microplate reader (Tecan).

qPCR

mRNA was isolated using the RNeasy mini kit (QIAGEN). The cDNA was synthesized using the PrimeScript RT reagent kit (Takara). qPCR was conducted using a SYBR Green PCR master mix kit (Takara) and an ABI 7900HT fast real-time PCR system (Applied Biosystems). mRNA expression levels of target genes were normalized to GAPDH and calculated by the $\Delta\Delta Ct$ method.

Western Blotting

Total cell lysates were harvested using radioimmunoprecipitation assay (RIPA) buffer (Thermo Fisher Scientific) supplemented with protease inhibitor cocktail (Roche). Protein concentrations were determined by a Pierce bicinchoninic acid (BCA) protein assay kit (Thermo Fisher Scientific). 15–30 μg of proteins were subjected to SDS-PAGE and immunoblotting.

ELISA

Cell-free supernatants of lentivirus-transduced mouse AT-MSCs were collected and kept in a refrigerator at $-80°C$ until measurement. CXCL9 secreted into the supernatants was quantified using a mouse CXCL9 ELISA kit (Abcam) according to the supplier's instructions.

Syngeneic Mouse Models and Administration of MSCs

CT26 and MC38 (wild-type, MHC class I-deficient sgB2m, and control sgLacZ) (0.5×10^6/mouse) cells were injected subcutaneously at the right lower flank of 8- to 8-week-old BALB/c and C57BL/6 mice, respectively. Tumors were treated when their size reached 0.5–0.7 cm in the largest diameter. Suspension of 5×10^5 AT-MSCs in 250 μL of PBS or 250 μL of PBS per animal was injected i.v. into the lateral tail vein for systemic administration. Tumors were measured every 3 days using a digital caliper, and the tumor volume was calculated using the following formula: $V = L \times W^2/2$, where L and W are the long and short diameters of tumor, respectively. TGI was calculated using the following formula:[50] $[(Ct - C0) - (Tt - T0)]/(Ct - C0) \times 100\%$, where Ct represents the mean tumor volume of the control group at a specific time (t), C0 represents the mean tumor volume of the control group at t0, Tt represents mean tumor volume of the treatment group at t, and T0 represents the mean tumor volume of the treatment group at t0. Mice were sacrificed when tumors reached 2 cm³ in volume or tumors became ulcerated or when mice became moribund.

Flow Cytometry

To characterize AT-MSCs, the adherent cells at the third to fourth passages were detached using 10 mM EDTA, then washed with PBS and stained with antibodies for FACS analysis.

To analyze tumor-infiltrating immune cells, subcutaneously implanted tumors were dissected and transferred into RPMI 1640 medium, disrupted mechanically with scissors, digested using a mouse tumor dissociation kit and a gentleMACS Octo Dissociator (Miltenyi Biotec) at 37°C, and dispersed through a 40-μm cell strainer (BD Biosciences). Single cells were further washed and stained with antibodies. Dead cells were excluded by staining with a Zombie fixable viability kit (BioLegend). To detect intracellular cytokine expression, separated cells were stimulated for 6 h with cell activation cocktail (BioLegend). Fluorescence data were acquired on a BD LSRFortessa cell analyzer (BD Biosciences) and analyzed using FlowJo software.

AOM/DSS-Induced Colorectal Tumor Model

Colitis-associated colon cancer was induced as previously described.[24,25] BALB/c mice were injected i.p. with the procarcinogen AOM (12.5 mg/kg of body weight; Sigma-Aldrich). After 1 week, mice received drinking water supplemented with 2.5% DSS (MP Biomedicals) for 7 days, followed by 2 weeks of regular water. The DSS treatment was repeated for two additional cycles, and mice were sacrificed after six injections of 0.5×10^6 AT-MSCs each in the tail vein, starting from the last week of the DSS treatment cycle. After treatment, colons were removed from mice, flushed with cold PBS, and opened longitudinally. Tumor size was measured using a digital caliper. Colon tissues were then fixed in 4% formalin solution (Sigma-Aldrich) and paraffin embedded. TGI was calculated using the following formula: $(Cn - Tn)/Cn \times 100\%$, where Cn represents the mean tumor number of the control group, and Tn represents the mean tumor number of the treatment group.

Immunohistochemistry and Immunofluorescence

Expression of Ki67 was assessed by immunohistochemistry using anti-Ki67 (Abcam) and detected using a diaminobenzidine (DAB) peroxidase substrate kit (Gene Tech, Shanghai). GFP, CD8a, and NKp46 were detected by immunofluorescence using anti-GFP (Abcam), anti-mouse CD8a (clone 53-6.7), and anti-mouse NKp46 (CD335) (clone 29A1.4) (BioLegend). Slides were mounted in anti-fade mounting medium with DAPI (Thermo Fisher Scientific) and visualized under a Nikon fluorescence microscope.

Statistical Analysis

All results are expressed as mean ± SEM. Differences were assessed by the Student's t test or, when means of more than two groups were compared, by two-way ANOVA followed by a Bonferroni multiple comparison test. Comparisons of survival curves were made using the log-rank (Mantel-Cox) test. Data analyses were performed with Prism software (GraphPad). Statistical significance was set at the level of $p < 0.05$.

Study Approval

All animal procedures were approved by the Institutional Animal Care and Use Committee of Shanghai Jiao Tong University (Shanghai, China).

SUPPLEMENTAL INFORMATION

Supplemental Information can be found online at https://doi.org/10.1016/j.ymthe.2020.08.005.

AUTHOR CONTRIBUTIONS

CONFLICTS OF INTEREST

The authors declare no competing interests.

ACKNOWLEDGMENTS

REFERENCES

1. Ribas, A., and Wolchok, J.D. (2018). Cancer immunotherapy using checkpoint blockade. Science 359, 1350–1355.

2. June, C.H., O'Connor, R.S., Kawalekar, O.U., Ghassemi, S., and Milone, M.C. (2018). CAR T cell immunotherapy for human cancer. Science 359, 1361–1365.

3. Pitt, J.M., Vétizou, M., Daillère, R., Roberti, M.P., Yamazaki, T., Routy, B., Lepage, P., Boneca, I.G., Chamaillard, M., Kroemer, G., and Zitvogel, L. (2016). Resistance mechanisms to immune-checkpoint blockade in cancer: tumor-intrinsic and -extrinsic factors. Immunity 44, 1255–1269.

4. Zou, W., Wolchok, J.D., and Chen, L. (2016). PD-L1 (B7-H1) and PD-1 pathway blockade for cancer therapy: mechanisms, response biomarkers, and combinations. Sci. Transl. Med. 8, 328rv4.

5. Peng, D., Kryczek, I., Nagarsheth, N., Zhao, L., Wei, S., Wang, W., Sun, Y., Zhao, E., Vatan, L., Szeliga, W., et al. (2015). Epigenetic silencing of T_H1-type chemokines shapes tumour immunity and immunotherapy. Nature 527, 249–253.

6. Nagarsheth, N., Peng, D., Kryczek, I., Wu, K., Li, W., Zhao, E., Zhao, L., Wei, S., Frankel, T., Vatan, L., et al. (2016). PRC2 epigenetically silences Th1-type chemokines to suppress effector T-cell trafficking in colon cancer. Cancer Res. 76, 275–282.

7. Pan, J., Burdick, M.D., Belperio, J.A., Xue, Y.Y., Gerard, C., Sharma, S., Dubinett, S.M., and Strieter, R.M. (2006). CXCR3/CXCR3 ligand biological axis impairs RENCA tumor growth by a mechanism of immunoangiostasis. J. Immunol. 176, 1456–1464.

8. Weber, J.S., Yang, J.C., Atkins, M.B., and Disis, M.L. (2015). Toxicities of immunotherapy for the practitioner. J. Clin. Oncol. 33, 2092–2099.

9. Johnson, D.B., Balko, J.M., Compton, M.L., Chalkias, S., Gorham, J., Xu, Y., Hicks, M., Puzanov, I., Alexander, M.R., Bloomer, T.L., et al. (2016). Fulminant myocarditis with combination immune checkpoint blockade. N. Engl. J. Med. 375, 1749–1755.

10. Moslehi, J.J., Salem, J.E., Sosman, J.A., Lebrun-Vignes, B., and Johnson, D.B. (2018). Increased reporting of fatal immune checkpoint inhibitor-associated myocarditis. Lancet 391, 933.

11. Shah, K. (2012). Mesenchymal stem cells engineered for cancer therapy. Adv. Drug Deliv. Rev. 64, 739–748.

12. Amara, I., Touati, W., Beaune, P., and de Waziers, I. (2014). Mesenchymal stem cells as cellular vehicles for prodrug gene therapy against tumors. Biochimie 105, 4–11.

13. Stuckey, D.W., and Shah, K. (2014). Stem cell-based therapies for cancer treatment: separating hope from hype. Nat. Rev. Cancer 14, 683–691.

14. Kern, S., Eichler, H., Stoeve, J., Klüter, H., and Bieback, K. (2006). Comparative analysis of mesenchymal stem cells from bone marrow, umbilical cord blood, or adipose tissue. Stem Cells 24, 1294–1301.

15. Ahmadian Kia, N., Bahrami, A.R., Ebrahimi, M., Matin, M.M., Neshati, Z., Almohaddesin, M.R., Aghdami, N., and Bidkhori, H.R. (2011). Comparative analysis of chemokine receptor's expression in mesenchymal stem cells derived from human bone marrow and adipose tissue. J. Mol. Neurosci. 44, 178–185.

16. Linch, S.N., McNamara, M.J., and Redmond, W.L. (2015). OX40 agonists and combination immunotherapy: putting the pedal to the metal. Front. Oncol. 5, 34.

17. Allen, F., Bobanga, I.D., Rauhe, P., Barkauskas, D., Teich, N., Tong, C., Myers, J., and Huang, A.Y. (2017). CCL3 augments tumor rejection and enhances CD8^{+} T cell infiltration through NK and CD103^{+} dendritic cell recruitment via IFNγ. OncoImmunology 7, e1393598.

18. Goswami, C.P., and Nakshatri, H. (2014). PROGgeneV2: enhancements on the existing database. BMC Cancer 14, 970.

19. Wu, Z., Huang, X., Han, X., Li, Z., Zhu, Q., Yan, J., Yu, S., Jin, Z., Wang, Z., Zheng, Q., and Wang, Y. (2016). The chemokine CXCL9 expression is associated with better prognosis for colorectal carcinoma patients. Biomed. Pharmacother. 78, 8–13.

20. Vigne, S., Palmer, G., Lamacchia, C., Martin, P., Talabot-Ayer, D., Rodriguez, E., Ronchi, F., Sallusto, F., Dinh, H., Sims, J.E., and Gabay, C. (2011). IL-36R ligands are potent regulators of dendritic and T cells. Blood 118, 5813–5823.

21. Wang, X., Zhao, X., Feng, C., Weinstein, A., Xia, R., Wen, W., Lv, Q., Zuo, S., Tang, P., Yang, X., et al. (2015). IL-36γ transforms the tumor microenvironment and promotes type 1 lymphocyte-mediated antitumor immune responses. Cancer Cell 28, 296–306.

22. Terzic, J., Grivennikov, S., Karin, E., and Karin, M. (2010). Inflammation and colon cancer. Gastroenterology 138, 2101–2114.e5.

23. Ullman, T.A., and Itzkowitz, S.H. (2011). Intestinal inflammation and cancer. Gastroenterology 140, 1807–1816.

24. Neufert, C., Becker, C., and Neurath, M.F. (2007). An inducible mouse model of colon carcinogenesis for the analysis of sporadic and inflammation-driven tumor progression. Nat. Protoc. 2, 1998–2004.

25. Thaker, A.I., Shaker, A., Rao, M.S., and Ciorba, M.A. (2012). Modeling colitis-associated cancer with azoxymethane (AOM) and dextran sulfate sodium (DSS). J. Vis. Exp. (67), 4100.

26. Garrido, F., Aptsiauri, N., Doorduijn, E.M., Garcia Lora, A.M., and van Hall, T. (2016). The urgent need to recover MHC class I in cancers for effective immunotherapy. Curr. Opin. Immunol. 39, 44–51.

27. Aptsiauri, N., Ruiz-Cabello, F., and Garrido, F. (2018). The transition from HLA-I positive to HLA-I negative primary tumors: the road to escape from T-cell responses. Curr. Opin. Immunol. 51, 123–132.

28. Rooney, M.S., Shukla, S.A., Wu, C.J., Getz, G., and Hacohen, N. (2015). Molecular and genetic properties of tumors associated with local immune cytolytic activity. Cell 160, 48–61.

29. Tumeh, P.C., Harview, C.L., Yearley, J.H., Shintaku, I.P., Taylor, E.J., Robert, L., Chmielowski, B., Spasic, M., Henry, G., Ciobanu, V., et al. (2014). PD-1 blockade induces responses by inhibiting adaptive immune resistance. Nature 515, 568–571.

30. Gajewski, T.F., Louahed, J., and Brichard, V.G. (2010). Gene signature in melanoma associated with clinical activity: a potential clue to unlock cancer immunotherapy. Cancer J. 16, 399–403.

31. Melero, I., Rouzaut, A., Motz, G.T., and Coukos, G. (2014). T-cell and NK-cell infiltration into solid tumors: a key limiting factor for efficacious cancer immunotherapy. Cancer Discov. 4, 522–526.

32. Dangaj, D., Bruand, M., Grimm, A.J., Ronet, C., Barras, D., Duttagupta, P.A., Lanitis, E., Duraiswamy, J., Tanyi, J.L., Benencia, F., et al. (2019). Cooperation between

constitutive and inducible chemokines enables t cell engraftment and immune attack in solid tumors. Cancer Cell 5, 885-90–.e10.

33. Emerson, D.A., and Redmond, W.L. (2018). Overcoming tumor-induced immune suppression: from relieving inhibition to providing costimulation with T cell agonists. BioDrugs 32, 221–231.

34. Cabo, M., Offringa, R., Zitvogel, L., Kroemer, G., Muntasell, A., and Galluzzi, L. (2017). Trial watch: immunostimulatory monoclonal antibodies for oncological indications. OncoImmunology 6, e1371896.

35. Rafiq, S., Yeku, O.O., Jackson, H.J., Purdon, T.J., van Leeuwen, D.G., Drakes, D.J., Song, M., Miele, M.M., Li, Z., Wang, P., et al. (2018). Targeted delivery of a PD-1-blocking scFv by CAR-T cells enhances anti-tumor efficacy in vivo. Nat. Biotechnol. 36, 847–856.

36. Swart, M., Verbrugge, I., and Beltman, J.B. (2016). Combination approaches with immune-checkpoint blockade in cancer therapy. Front. Oncol. 6, 233.

37. Vilgelm, A.E., Johnson, D.B., and Richmond, A. (2016). Combinatorial approach to cancer immunotherapy: strength in numbers. J. Leukoc. Biol. 100, 275–290.

38. Zhang, S., Kohli, K., Black, R.G., Yao, L., Spadinger, S.M., He, Q., Pillarisetty, V.G., Cranmer, L.D., Van Tine, B.A., Yee, C., et al. (2019). Systemic interferon-γ increases MHC class I expression and T-cell infiltration in cold tumors: results of a phase 0 clinical trial. Cancer Immunol. Res. 7, 1237–1243.

39. Tian, K., Yang, S., Ren, Q., Han, Z., Lu, S., Ma, F., Zhang, Z., and Han, Z. (2010). p38 MAPK contributes to the growth inhibition of leukemic tumor cells mediated by human umbilical cord mesenchymal stem cells. Cell. Physiol. Biochem. 26, 799–808.

40. Lalu, M.M., McIntyre, L., Pugliese, C., Fergusson, D., Winston, B.W., Marshall, J.C., Granton, J., and Stewart, D.J.; Canadian Critical Care Trials Group (2012). Safety of cell therapy with mesenchymal stromal cells (SafeCell): a systematic review and meta-analysis of clinical trials. PLoS ONE 7, e47559.

41. Peeters, C.M., Leijs, M.J., Reijman, M., van Osch, G.J., and Bos, P.K. (2013). Safety of intra-articular cell-therapy with culture-expanded stem cells in humans: a systematic literature review. Osteoarthritis Cartilage 21, 1465–1473.

42. Serhal, R., Saliba, N., Hilal, G., Moussa, M., Hassan, G.S., El Atat, O., and Alaaeddine, N. (2019). Effect of adipose-derived mesenchymal stem cells on hepatocellular carcinoma: in vitro inhibition of carcinogenesis. World J. Gastroenterol. 25, 567–583.

43. Zakaria, N., and Yahaya, B.H. (2020). Adipose-derived mesenchymal stem cells promote growth and migration of lung adenocarcinoma cancer cells. Adv. Exp. Med. Biol. Published online January 9, 2020. 10.1007/5584_2019_464.

44. Yulyana, Y., Ho, I.A., Sia, K.C., Newman, J.P., Toh, X.Y., Endaya, B.B., Chan, J.K., Gnecchi, M., Huynh, H., Chung, A.Y., et al. (2015). Paracrine factors of human fetal MSCs inhibit liver cancer growth through reduced activation of IGF-1R/PI3K/Akt signaling. Mol. Ther. 23, 746–756.

45. Han, I., Yun, M., Kim, E.O., Kim, B., Jung, M.H., and Kim, S.H. (2018). Retracted. Stem Cell Res. Ther. 9, 354.

46. Menge, T., Gerber, M., Wataha, K., Reid, W., Guha, S., Cox, C.S., Jr., Dash, P., Reitz, M.S., Jr., Khakoo, A.Y., and Pati, S. (2013). Human mesenchymal stem cells inhibit endothelial proliferation and angiogenesis via cell-cell contact through modulation of the VE-cadherin/β-catenin signaling pathway. Stem Cells Dev. 22, 148–157.

47. Reinshagen, C., Bhere, D., Choi, S.H., Hutten, S., Nesterenko, I., Wakimoto, H., Le Roux, E., Rizvi, A., Du, W., Minicucci, C., and Shah, K. (2018). CRISPR-enhanced engineering of therapy-sensitive cancer cells for self-targeting of primary and metastatic tumors. Sci. Transl. Med. 10, eaao3240.

48. Sanjana, N.E., Shalem, O., and Zhang, F. (2014). Improved vectors and genome-wide libraries for CRISPR screening. Nat. Methods 11, 783–784.

49. Araña, M., Mazo, M., Aranda, P., Pelacho, B., and Prosper, F. (2013). Adipose tissue-derived mesenchymal stem cells: isolation, expansion, and characterization. Methods Mol. Biol. 1036, 47–61.

50. Hossain, D.M.S., Javaid, S., Cai, M., Zhang, C., Sawant, A., Hinton, M., Sathe, M., Grein, J., Blumenschein, W., Pinheiro, E.M., and Chackerian, A. (2018). Dinaciclib induces immunogenic cell death and enhances anti-PD1-mediated tumor suppression. J. Clin. Invest. 128, 644–654.